17th International Conference on Metal Forming, Metal Forming 2018, 16-19 September 2018, Toyohashi, Japan

Influence of choked angle of bearing channel on profile grain structure during multi-hole extrusion of aluminum alloy

Soeren Mueller[a], Vidal Sanabria[b],*

[a]Extrusion Research and Development Center, Technische Universität Berlin, Berlin 13355, Germany
[b]INGWERK GmbH, 13355 Berlin, Germany

Abstract

Direct extrusion of aluminum alloy EN AW-6060 was carried out applying a four-hole die with pair-wise parallel and choked long channels. Due to the dissimilar friction inside parallel and choked channels profiles with different length were extruded simultaneously. In order to investigate the grain structure evolution along the whole extrusion process, multiple sections from the beginning to the end of the products were analyzed. Macroetch tests revealed unrecrystallized fibrous, fully recrystallized as well as partially recrystallized grains. The results also showed an axial and radial grain structure variation. At the beginning of the extrudates unrecrystallized fibrous microstructure was observed, while a fully recrystallized structure characterized the end of the products. Additionally, finer grains were present at the surface, whereas coarser grains were found in the center of the extrudates. Finally, numerical simulations allowed estimating the temperature, strain and strain rate evolution along the whole product length. Thus, a correlation between the extrusion parameters, deformation conditions and the grain structure was obtained.

Keywords: Direct extrusion; Aluminum alloy; Multi-hole die; Friction; Microstructure evolution; FE Simulation

1. Introduction

The grain structure of extruded aluminum profiles is classified basically in unrecrystallized fibrous, fully recrystallized and partially recrystallized [1, 2]. An unrecrystallized fibrous structure is preferred because it improves

---

* Corresponding author. Tel.: +49-30-46069169 ; fax: +49-30-46069168 .
  E-mail address: vidal.sanabria@ingwerk.com

the mechanical properties. On the other hand, large recrystallized grains reduce the machinability and stress corrosion resistance. Their presence at the surface can generate bending failure and poor decorative finish [3]. The influence of the extrusion parameters on the final microstructure has widely been studied. Parson and co-workers suggested that the fraction of recrystallized grains as well as the recrystallized grain size were closely related to ram speed, billet temperature and extrusion ratio [1]. They found that the ram speed was the main factor controlling grain size and shape, and that the exit temperature was not a good indicator of grain structure. Contrary, another investigation found that the profile exit temperature highly affects the recrystallization process [3]. More recent investigations have shown the influence of the temperature and speed of the deformation on the microstructure evolution of the aluminum alloy [4, 5]. The results showed smaller grain size at higher strain rates, but larger grains at higher temperatures. During large plastic deformation of aluminum alloy geometric dynamic recrystallization gDRX takes place [6]. The grains are elongated and their thickness becomes equal to the subgrain size. This process is also called grain impingement. At higher rates of deformation less dislocations are annihilated and therefore are arranged in smaller subgrains. At higher temperatures the annihilation process is more efficient. Due to the higher mobility of dislocations hence larger grains are produced. According to the stored energy and the local temperature the grains can subsequently statically recrystallize and grow.

In this work, microstructure of selected profiles extruded through a multi-hole die in a previous work [7] were investigated. Different profile microstructures were expected, since dissimilar extrudate speeds were obtained. Profile sections along the complete length were analysed in order to describe grain structure evolution in the radial and longitudinal direction. Moreover, the microstructure inside bearing channels was also investigated. In addition, numerical simulation of the whole extrusion process was carried out to analyze the distribution of the temperature, strain and strain rate inside the bearing channels. Finally, experimental and numerical results were used to analyze the evolution of the grain structures along the extrudates.

2. Experimental procedure

A direct extrusion experiment was carried out at the Extrusion Research and Development Center (ERDC) at the TU of Berlin. Its 8 MN horizontal press allows measuring the container and die force simultaneously. The total extrusion force is the sum of the container and die forces. A billet with diameter 137 mm and length 355 mm was machined from the cast and homogenized aluminum alloy EN AW-6060 provided by Otto Fuchs KG (Fig. 1(a)). The trial was carried out with a four-hole die with interchangeable inserts (Fig. 1(b)). Inserts with the same configuration were placed pair-wise in the die. Thus, the inserts 1 and 4 were manufactured with parallel channels and the inserts 2 and 3 with +0.5° (α) choked channels (Fig. 1(b)). All inserts were designed with the same pocket configuration, inlet diameter (20 mm) and length of the bearing channels (Fig. 1(c)). Because of the choked angel of the inserts 2 and 3 the outlet diameter of the bearing channel is 19.82 mm. Moreover, the billet was inductively heated to 460 °C while container, punch and die were heated to 470 °C. The billet was extruded with a ram speed of 4 mm/s approximately. After extrusion die, discard (20 mm) and profiles were cooled in air to avoid any relative movement between the aluminum and the bearing channel. After cooling the discard was machined off and could be separated the aluminum. The filled inserts were carefully extracted. Subsequently, each insert was lengthwise cut by means of wire-cut erosion. Finally, one half was used to investigate the contact area of the bearing channel and the other half to analyze the aluminum microstructure. Additionally, many sections of the profiles were cut, ground and macroetched to investigate the evolution of the grain structure during the extrusion process.
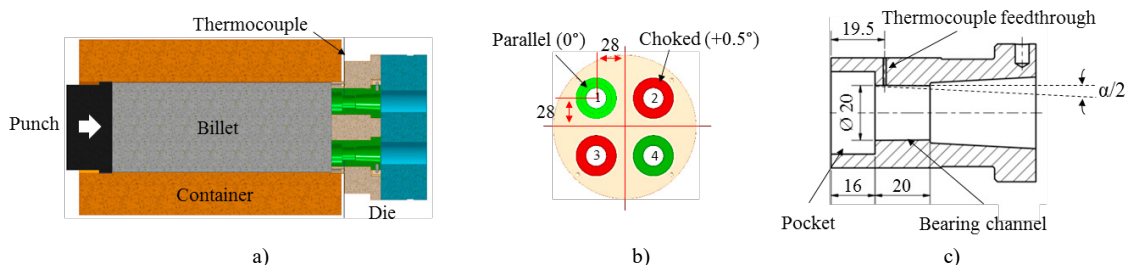

Fig. 1. Multi-hole extrusion with long bearing channels. (a) Arrangement during direct extrusion; (b) position of inserts in multi-hole die; (c) insert configuration.

3. Experimental results

3.1. Multi-hole extrusion

During the experimental trial the extrusion forces and profile temperatures were measured and recorded (Fig. 2(a)). Load cells placed in the 8 MN press allowed independent measuring of the container and die forces. Additionally, the profile temperature of all extrudates was simultaneously meassured through thermocouples placed inside the bearing channel (Fig. 1(c)). The total extrusion force increased to a maximum value of 5.1 MN when the pockets and bearing channels were filled with aluminum (Point **a** in Fig. 2(a)). At this point the temperature difference of the aluminum surfaces inside disimilar bearing channels was very low (5±3 °C), due to their comparable deformation history. Subsequently, the total force decreased progressively due to the reduction of the container force (friction between billet and container). Moreover, the temperature inside the bearing channel increased to a maximal value of 523±4 °C in parallel (0°) and 510±2 °C in choked (+0.5°) channels respectively. Through the single profile length and the extrusion time (76 s) the individual average speed could be estimated. Thus, the profile speeds were 64 mm/s and 69 mm/s through parallel channels and 30 mm/s through choked channels. The disimilar profile speed generated different strain rate and heat rate generation. For this reason higher tempertaures were measured in bearing channels with higher profile speed.

Fig. 2(b) and 2(c) show sections of inserts 1 (0°) and 3 (+0.5°) after extrusion respectively. Based on the topography and color of the bearing channels, sticking and slipping zones can be identified [8]. An aluminum colored layer was observed in the inlet of the parallel channel (Fig. 2(b)). This layer remained stuck after removing the aluminum workpiece suggesting a sticking friction. This zone was followed by aluminum stripes in the extrusion direction, which clearly confirmed slipping friction [8]. Furthermore, the dark color in the inlet of the choked channel (Fig. 2(c)) is the iron oxide layer, which was generated during the die heating at 470 °C. It means that the iron oxide was covered by an aluminum layer which remained adhered during the whole extrusion process. Probably this thick oxide layer avoided the intimate contact between aluminum and steel and therefore, they were easily separated. A longer sticking zone in choked channels generated a higher friction and therefore a lower profile speed than in parallel channels. A more detailed description of the contact friction mechanisms inside the bearing channels have been reported in a previous investigation [7].
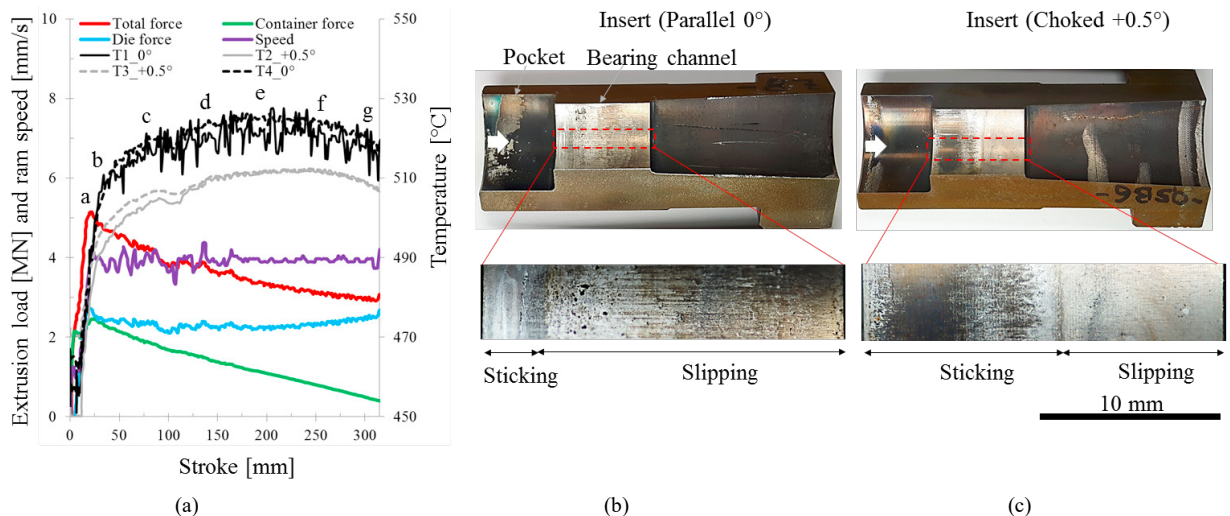

Fig. 2. (a) Extrusion force and temperature inside bearing channel; section of (b) parallel and (c) choked +0.5° bearing channels.

3.2. Microstructure analysis

In order to investigate the grain structure evolution along the extudates several profile sections were metallographically analyzed. Letters **a** to **g** in Fig. 2(a) depict the selected stroke positions where taken. Since the profiles were extruded with dissimilar speeds, the studied sections were located at different positions along the

extrudates. Table 1 shows the position of studied sections extracted from profiles extruded through the inserts 1 (0°) and 3 (+0.5°) measured from the front end, as well as the bearing temperature and relative ram stroke.

Table 1. Information of studied sections cut from selected extrudates.

			a	b	c	d	e	f	g
Insert 1 (Profile 1)	64	Length [mm]	1	65	960	1920	2880	3840	4880
(Parallel °0)	mm/s	Temp [°C]	489	508	516	517	523	520	514
Insert 3 (Profile 3)	30	Length [mm]	1	30	435	870	1305	1740	2245
(Choked +0.5°)	mm/s	Temp [°C]	488	497	506	510	511	511	505
Ram	4 mm/s	Stroke [mm]	22	25	80	138	196	254	316

Similar microstructures were observed in profiles extruded through channels with the same configuration. Fig. 3 shows the evolution of the grain structure of profiles extruded through the channels 1 (0°) and 3 (+0.5°). According to the results a microstructure gradient occurred not only across the profiles but also along the extrusion direction. At the front end (section **a**) of profile 1 an unrecrystallized fibrous structure with coarse grains at the edge was observed. Moreover, fibrous structure as well as large grains were found in the center of section **b**, whereas fine grains at the edge were observed. The sections **c** to **g** were characterized by equiaxial grains in the center (zone I), finer grain size at the edge (zone III) and even much finer in zone II (Fig. 3). As well as in section **a** of profile 1, unrecrystallized fibrous structure with coarse grains at the edge were found in section **a** of profile 3. Furthermore, coarse grains appeared in zone II of section **b**. Zones I, II and III were also observed in sections **c-g** of profile 3, however they had clearly higher grain size than those in profile 1.

Fig. 4a and 4b show the thickness variation of the different zones found in profiles 1 and 3 respectively. Thus, the average thickness of zones I, II and III was 10.4 mm, 2.3 mm and 2.5 mm for profile 1 and 11.1 mm, 2.3 mm and 2.2 mm for profile 3 correspondingly. In addition, the grain size in each mentioned zones was also measured. Fig. 4c depicts the evolution of grain size of zones I and III along profiles 1 and 3. A significant grain size difference between both profiles could be observed. In profile 1 the grain size average was 600 µm and 300 µm for zones I and III, while 1800 µm and 560 µm was measured in profile 3.
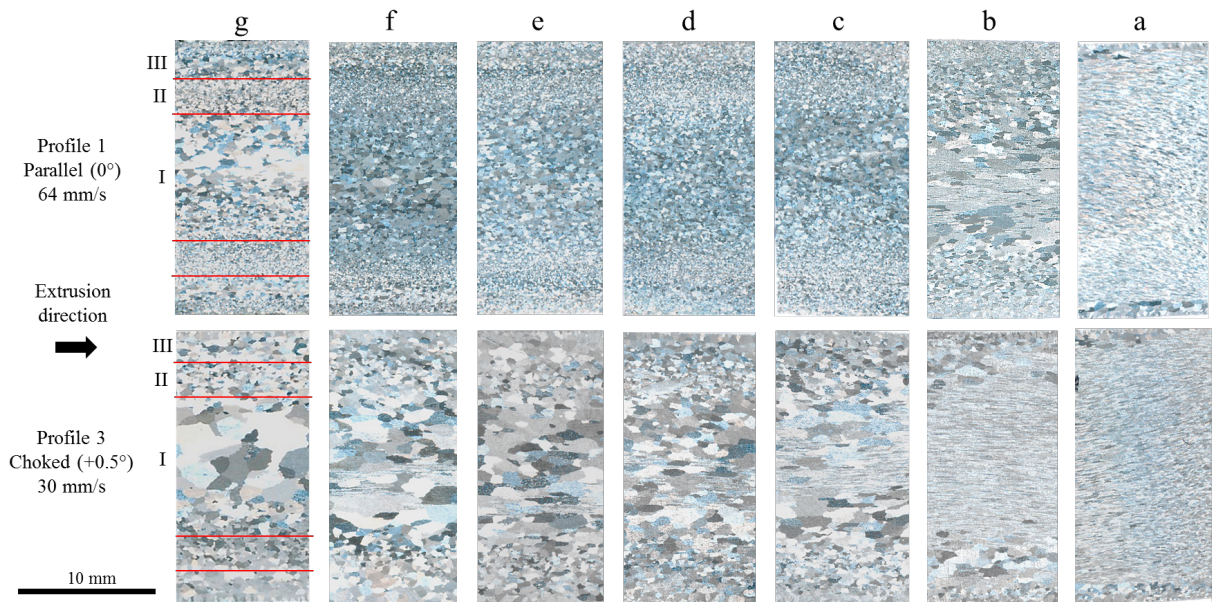

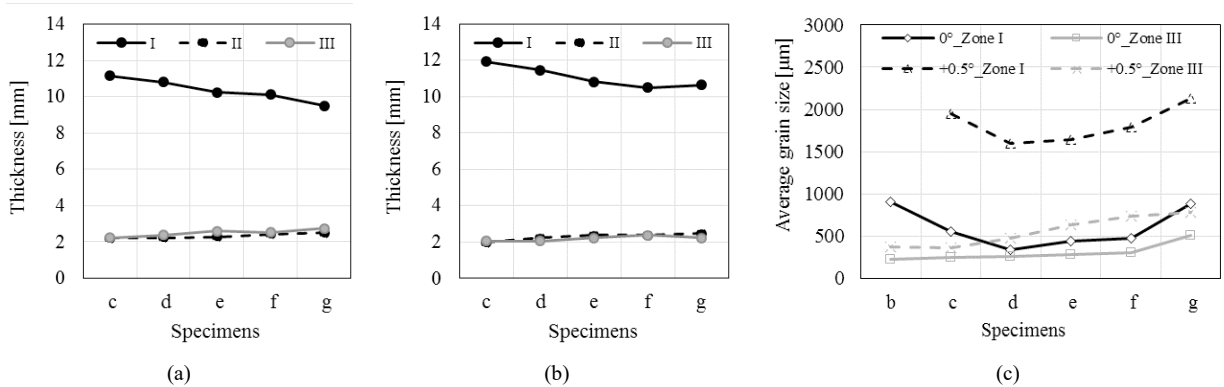Fig. 3. Microstructure of profile extruded through insert 1 (parallel 0°).

Fig. 4. Thickness evolution of different zones inside profiles extructed through (a) insert 1 (parallel 0°) and (b) the insert 3 (choked +0.5°); (c) average grane size of zones I and III.

4. Numerical analysis

The direct multi-hole extrusion was simulated, applying the FEM-based software DEFORM 3D. The billet was meshed and treated as rigid plastic, while die, container and punch were considered as rigid objects and were not meshed. Thus, plastic deformation and heat transfer were only simulated in the workpiece (billet). Hot compression tests of the aluminum alloy EN AW-6060 at the Gleeble 3800 were carried out at different strain rates (0.1 – 10 1/s) and temperatures (300-500 °C). The flow stress was calculated using the Garofalo or Zener-Hollomon relationship ($\alpha = 0.0265 \text{MPa-1}$, A = 2E+14 1/s, n = 5.3, and ΔH = 203800 J/mol), which is only related to strain rate and temperature $k_f(T, \dot{\varepsilon})$. Since state variables such as strain, strain rate and temperature inside the bearing channels had to be analyzed for all studied sections (a-g), the 3D simulation of the whole extrusion process was performed. Almost 30 days were needed to complete the whole numerical simulation. Additionally, the heat transfer coefficient between the workpiece and the tools was set constant at 7000 W/m^{2}K. The Tresca model was selected to establish the friction relationship between the workpiece and the tools. Sticking friction was set in the inlet of the bearing channels (2 mm for parallel, 11 mm for choked channels). Furthermore, the friction factors m = 0.2 and m = 0.7 were set in the outlet of the parallel and choked channels respectively. Hence, sticking and slipping friction mechanisms observed inside bearing channels (Fig. 2c, 2c) could be reproduced.

Fig. 5a compares the experimental and simulated extrusion forces during the complete ram stroke. The simulation started with filled pockets and bearing channels and therefore, the estimated curves did not begin at stroke 0 mm but at stroke 22 mm. The friction force between container and billet (container force) was exactly reproduced with the numerical simulation. Since the values of the deformation parameters inside the container ($\dot{\varepsilon}$ = 0.2 1/s, T = 475 °C) were inside the range tested with the hot compression test, a good estimation of the container force was expected. On the other hand, the predicted die force was around 30 % higher than the measured value. Inaccurate estimation of flow stress inside the bearing channels could have caused this relevant difference. Under certain conditions of temperatures and strain rate softening effects can occurr, which cannot be reproduced with the Garafalo formulation used in this numerical model. Moreover, the strain rate at the sticking friction zones in the inlet of the bearing channels is much higher (100 %– 300 %) than this tested in the hot compression test (Fig. 6). For this reason an inaccurate estimation of the flow stress in the sticking zones can also be possible.

Fig. 5(b) shows the experimental and simulated temperatures on the bearing channel during the whole extrusion process. The measured temperature in the steady state zone (after stroke 100 mm) was well simulated, however low values were obtained in the first part of the curve. A higher simulated stress inside bearing channels increased the local temperature as observed in the first 100 mm of stroke (Fig. 5(b)). Additionally, the complex heat transfer between workpiece and tools cannot accurately be simulated with a simple heat transfer coefficient. In order to obtain a better estimation of the temperature evolution the heat transfer coefficient should be simulated at least as function of normal pressure. Moreover, the heat transfer through die and die support should be also simulated.
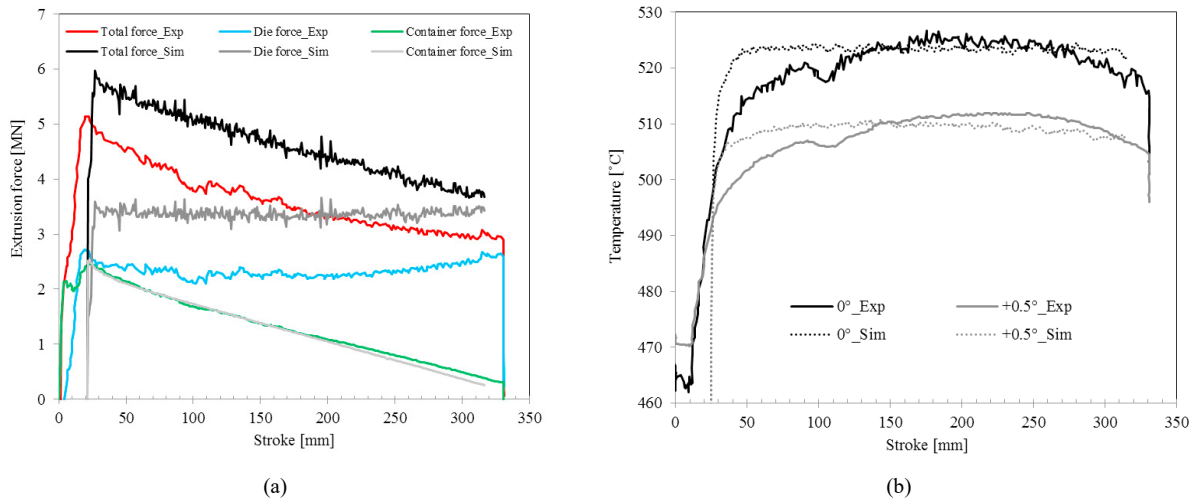
Fig. 5. Validation of numerical simulation. (a) Extrusion force; (b) temperature evolution inside bearing channel.

The numerical simulation of the whole extrusion process provided relevant information about the evolution of the strain, strain rate and temperature. Special emphasis was given to the analysis inside the inserts (pocket and bearing channels), because in this area most of plastic deformation and therefore the greatest heat generation occurred. Thus, simulation results could be used to understand how the observed microstructure was originated. Fig. 6 shows the grain structure and estimated strain rate distribution inside the inserts 1 and 3, as well as the microstructure of both profiles at the section **d**. Different deformation history generated dissimilar grain structures as observed inside the inserts. Dotted lines delineate different zones which have clearly different grain sizes and structures. Hence, the mentioned three zones (I, II and III) observed along the profile (Fig. 3) seem to be related to the same zones inside the bearing channel. Thus, the deformation inside the pocket and bearing channel is closely related to the grain structure inside the extrudates. Dissimilar length of sticking area inside the bearing channels produced different material flows and product speeds. The sticking area and the generated dead zone could be identified inside parallel channels (Fig. 6(a)) and choked channels (Fig. 6(b)). Below the dead zone a high shear deformation took place (zone III) but decreased toward the center (zone I) where the material flowed faster. This radial variation of the deformation was corroborated by the strain rate distribution of Fig. 6, which scale bar was set to a maximum value of 15 for a better presentation. A more detailed description of the state variables inside the bearing channels is presented in Fig. 7. True strain, strain rate and temperature across the bearing channels 1 (0°) and 3 (+0.5°) were compiled at a position of 4 mm from the inlet and four selected profile sections (**a**, **c**, **e** and **g**). Thus, the microstructure evolution observed in Figs. 3 and 6 can better be analyzed.
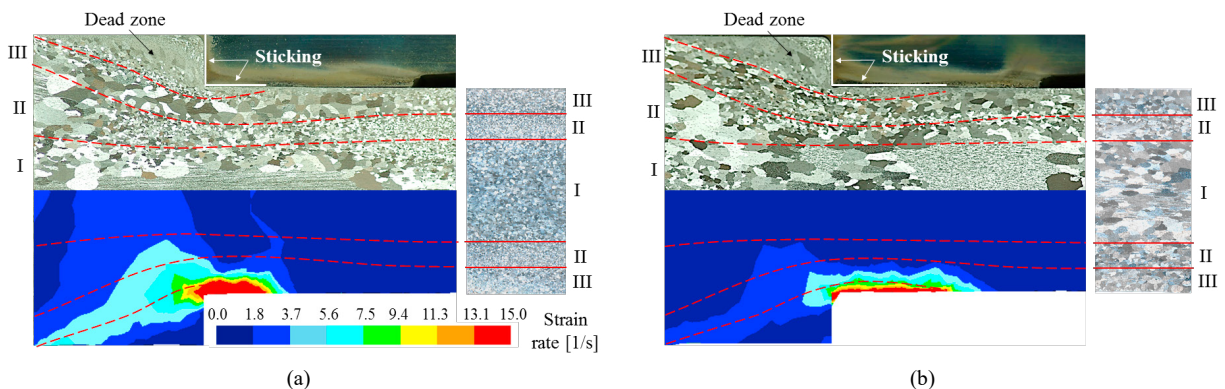

Fig. 6. Relation between grain structure and simulated strain rate inside (a) insert 1 (parallel 0°) and (b) insert 3 (choked +0.5°).
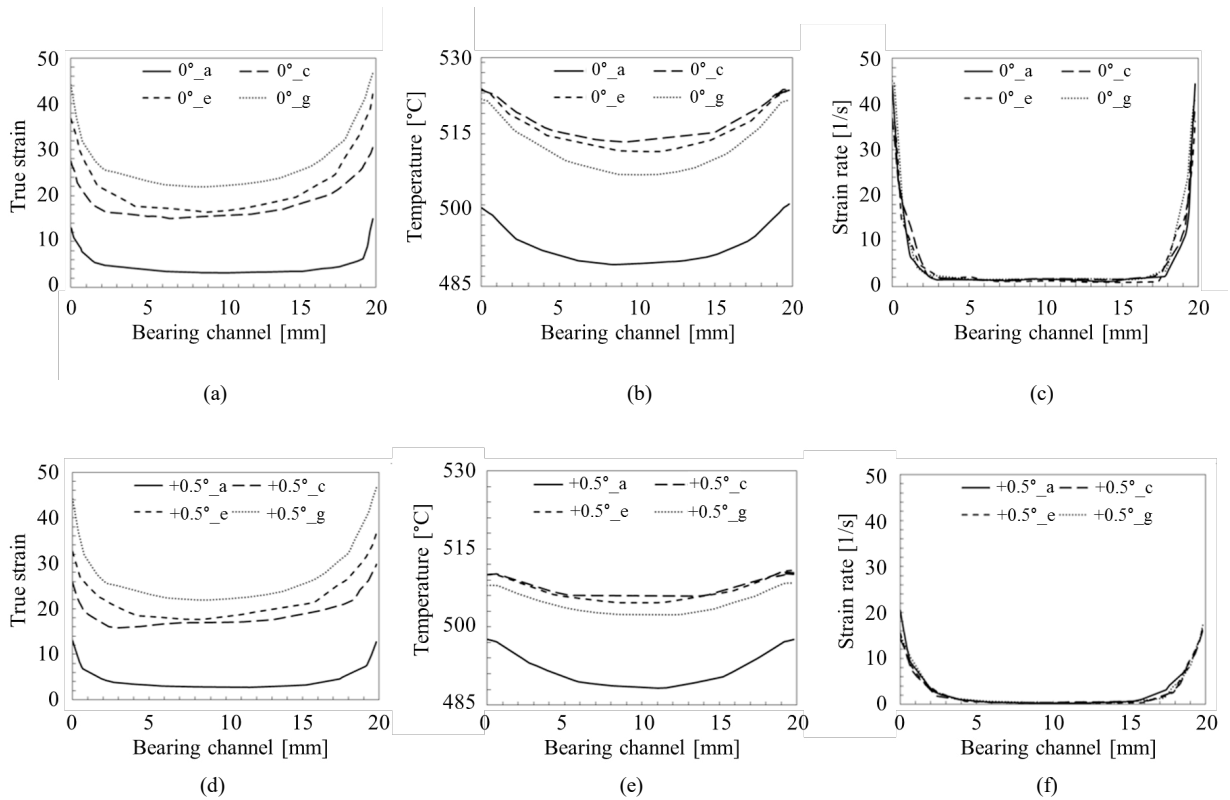
Fig. 7. Simulation results across bearing channel 4 mm from inlet. True strain, strain rate and tempertaure distribution across parallel 0° (a,b,c) and choked +0.5° (d,e,f) bearing channels respectively.

The final grain structure observed in Figs. 3 and 6 is not only the result of the restoration mechanisms during the extrusion (dynamic), but also those after the deformation (static). During the extrusion process dynamic recovery (DRV) and geometric dynamic recrystallization (gDRX) or grain dividing (gDRV) took place. Moreover, after extrusion static recrystallization and grain growth occurred.

At the front end of both profiles (section **a**) the original dendritic grains were elongated during the initial deformation to form the so called fibrous structure. The strain at the center ($\varepsilon_{0°} \approx 3.2$ and $\varepsilon_{+0.5°} \approx 2.8$) was lower than the critical value for static recrystallization and therefore, remained unchanged even after extrusion (Fig. 7(a), 7(d)). On the other hand, a higher strain ($\varepsilon \approx 12$) and higher temperature (~490 °C, Table 1) at the surface were enough to generate local recrystallization (Fig. 7(b), 7(e)). A considerable microstructure difference was noticed between profiles 1 and 3 from section **b**. In profile 1 the section **b** consisted of a mixture of fibrous and large grains in the center and fines grains at the surface. Due to a slight increase of the strain in the center a higher stored energy in presence of a higher temperature produced a selective static recrystallization and grain growth during the cooling phase. Toward the surface of this section the grain sizes became smaller due to the higher strain rate (Fig. 7(c)). At higher strain rates less dislocations are annihilated and they are arranged in smaller subgrains. As a result, smaller equiaxed grains are generated during geometric dynamic recrystallization (gDRX) as observed in the surface of sections **b** to **g** of profile 1 [9,10,11]. From section **c** no fibrous structure was found in the center but equiaxed grains due to a higher strain than in section **b** (Fig. 7(a)). At the edge, the grains were smaller than the center due to their higher strain rate as explained in section **b**. Contrary to section **b**, the grain size of the zone II was smaller than the zone III (Fig. 3). It could be due to the slightly higher temperature in the zone III (Fig. 7(b)). At higher temperatures the dislocation movements are more easily annihilated and therefore, larger subgrains are formed [12]. Subsequently bigger grains are formed during gDRX as also found in section **c**. Section **d** and **e** were similar to **c**. Finally, in the sections **f** and **g** the grains were bigger than in previous sections mainly because these sections were additionally heated by means of thermal

conduction from the die assembly still in contact during the air cooling process. In profile 3 the mixture of fibrous structure and large grains in the center was observed from the section **b** to **f**. It suggests that the fibrous structure remained during extrusion and the large and abnormal grains were generated during static recrystallization and grain growth. Due to the higher temperature in the section **g** no fibrous structure was observed, but full statically recrystallized. Similar to the profile 1, in profile 3 finer grains were found in zone II than in zone III, although higher strain rate was present in zone III. As explained above, the higher temperature at the edge facilitated the formation of larger recrystallized grains and possible grain growth. In general, a finer grain structure was produced in profile 1 due to the higher strain rate (Fig. 7(c), 7(f)).

5. Conclusions

The aluminum alloy EN AW-6060 was extruded applying a four-hole die with pair-wise parallel and choked long channels. The direct extrusion was carried out with a ram speed of 4 mm/s. Due to the dissimilar channel angle different friction behavior was generated. Thus, profiles extruded through parallel channels flowed faster (64-69 mm/s) than those through choked (30-31 mm/s). The different material flow and the measured temperature inside parallel and choked channels generated dissimilar grain structures. It was observed that the speed and the temperature inside the bearing channels (high deformation zone) were the most influential parameters to define the product microstructure. The product speed should not be taken as reference, but the strain rate inside the bearing channel. Three zones with dissimilar grain size were clearly identified inside the bearing channels as well as in the extrudates. Due to the higher strain rate near to the sticking friction zone, finer grains were observed at the extrudate surface. The microstructure observed in profile extruded at 64 mm/s suggested that geometric dynamic recrystallization and additionally grain growth took place. On the other hand, fibrous structure with static recrystallization and abnormal grain growth was considered in the center of the slower extrudate. Numerical results contributed to the understanding of the dynamic and static restoration of the microstructure. The strain distribution at the front end of the profiles allowed to explain the fibrous structure in both profiles. Moreover, strain rate gave significant information to delineate the grain structures from the center to the profile surface. Finally, the temperature evolution in the radial and longitudinal direction clarified different grain sizes in recrystallized structures.

References

[1] N. Parson, S. Barker, A. Shalanski, C. Jowett, Control of grain structure in Al-Mg-Si extrusions, Proceedings of the Eighth International Aluminum Extrusion Technology Seminar, Orlando, Florida, USA, 1 (2004) 11–21.
[2] A. Ockewitz, D. Sun, F. Andrieux, S. Mueller, Simulation of hot extrusion of an aluminium alloy with modeling of microstructure, Key Engineering Materials, 491 (2012) 257–264.
[3] E. Sweet, S. Caraher, N. Danilova, X. Zhang, Comalco aluminium limited, effects of extrusion parameters on coarse grain surface layer in 6xxx series extrusions, Proceedings of the Eighth International Aluminum Extrusion Technology Seminar, Orlando, Florida, USA, 1 (2004) 115–126.
[4] V. Sanabria, S. Mueller, W. Reimers, Microstructure evolution of friction boundary layer during extrusion of AA 6060, Procedia Engineering, 81 (2014) 586–591.
[5] V. Sanabria, S. Mueller, Influence of temperature and sliding speed on the subsurface microstructure evolution of EN AW-6060 under sticking conditions, AIP Conference Proceedings 1896, 140012, 1 (2017) 1–6.
[6] F.J. Humphreys, M. Hatherly, Recrystallization and Related Annealing Phenomena, Elsevier, Second edition, Oxford, U.K, (2004).
[7] V. Sanabria, S. Gall, S. Mueller, Friction behavior in long bearing channels during aluminum extrusion; experimental and numerical investigation, Proceedings of the Eleventh International Aluminum Extrusion Technology Seminar, 1 (2016) 703–714.
[8] H. Valberg, T. Malvik, An experimental investigation of the material flow inside the bearing channel in aluminium extrusion, International Journal of Materials and product Technology, 9 (1994) 428–463.
[9] M. Schikorra, L. Donati, L. Tomesani, A. Tekkaya, Microstructure analysis of aluminium extrusion: Prediction of microstructure on AA6060 alloy, Journal of Mechanical Processing Technology, 201 (2008) 156–162.
[10] T. Kayser, B. Klusemann, H. Lambers, H. Maier, B. Svendsen, Characterization of grain microstructure development in the aluminium alloy EN AW-6060 during extrusion, Material Science and Engineering: A, 527 (2010) 6568–6573.
[11] S. Gourdet, H. McQueen, High temperature deformation of 6060 aluminium alloy, Ibid, 326 (1999) 575–582.
[12] H. McQueen, J. Jonas, Plastic deformation of materials, Treatise on material science and technology, Akad. Press, New York, 6 (1975) 393–493.